

Zeitschrift: IABSE reports = Rapports AIPC = IVBH Berichte

Band: 54 (1987)

Artikel: Analysis of reinforced concrete structures in design applications

Autor: Isenberg, Jeremy / Millavec, William

DOI: <https://doi.org/10.5169/seals-41962>

Nutzungsbedingungen

Die ETH-Bibliothek ist die Anbieterin der digitalisierten Zeitschriften auf E-Periodica. Sie besitzt keine Urheberrechte an den Zeitschriften und ist nicht verantwortlich für deren Inhalte. Die Rechte liegen in der Regel bei den Herausgebern beziehungsweise den externen Rechteinhabern. Das Veröffentlichen von Bildern in Print- und Online-Publikationen sowie auf Social Media-Kanälen oder Webseiten ist nur mit vorheriger Genehmigung der Rechteinhaber erlaubt. [Mehr erfahren](#)

Conditions d'utilisation

L'ETH Library est le fournisseur des revues numérisées. Elle ne détient aucun droit d'auteur sur les revues et n'est pas responsable de leur contenu. En règle générale, les droits sont détenus par les éditeurs ou les détenteurs de droits externes. La reproduction d'images dans des publications imprimées ou en ligne ainsi que sur des canaux de médias sociaux ou des sites web n'est autorisée qu'avec l'accord préalable des détenteurs des droits. [En savoir plus](#)

Terms of use

The ETH Library is the provider of the digitised journals. It does not own any copyrights to the journals and is not responsible for their content. The rights usually lie with the publishers or the external rights holders. Publishing images in print and online publications, as well as on social media channels or websites, is only permitted with the prior consent of the rights holders. [Find out more](#)

Download PDF: 01.07.2025

ETH-Bibliothek Zürich, E-Periodica, <https://www.e-periodica.ch>

Analysis of Reinforced Concrete Structures in Design Applications

Analyse de structures en béton armé et application dans des projets

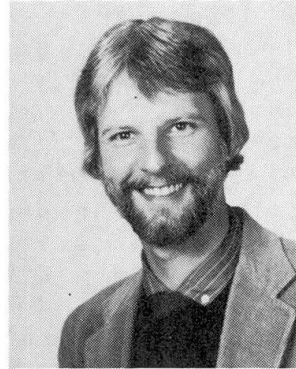
Betrachtungen von Stahlbetontragwerken beim Entwurfsprozess

Jeremy ISENBURG

Principal
Weidlinger Associates
Palo Alto, CA, U.S.A.



Jeremy Isenberg received BS and PhD degrees from Stanford and Cambridge Universities, respectively. A consulting engineer, he has worked in numerical methods applied to soil/structure interaction and reinforced concrete under earthquake and blast loading.



William Millavec received his BS and MS degrees in civil engineering from Case Western Reserve University. He has applied numerical methods to investigate and evaluate the survivability of soil/structure systems subjected to blast loading.

William MILLAVEC

Senior Res. Eng.
Weidlinger Associates
Palo Alto, CA, U.S.A.

SUMMARY

Design of complicated reinforced concrete structures can be effectively supported by finite element analysis using 32 bit minicomputers with multiple interactive terminals and batch communication to mainframe computers and graphics terminals. Multi-surface, cap-type constitutive models are used in an explicit, time-marching finite element computer program whose application in a design support example is illustrated.

RÉSUMÉ

Le projet de structures en béton armé compliquées peut être étudié au moyen d'analyses par éléments finis sur des mini-ordinateurs avec des terminaux multiples interactifs et en communication 'batch' avec de grands ordinateurs et des terminaux graphiques. Des modèles constitutifs multi-surfaces et 'cap-type' peuvent être utilisés dans un programme d'ordinateur avec des éléments finis. Un exemple d'application est donné.

ZUSAMMENFASSUNG

Entwurf und Berechnung komplizierter Stahlbetonkonstruktionen können hilfreich unterstützt werden, wenn man von Finite-Elemente-Programmen auf einem 32-bit-Minicomputer mit mehrfachen interaktiven Arbeitsstationen und Zugriff auf einen Zentralrechner und graphische Stationen Gebrauch macht. Materialgesetze mit mehrfachen, nach aussen offenen, Bruchgrenzflächen werden in einem expliziten, zeitgesteuerten Finite-Elemente-Programm benutzt, deren Anwendung in einem Beispiel gezeigt wird.



1. INTRODUCTION

Dynamic, nonlinear analysis has only recently gained a role in design of reinforced concrete structures to resist earthquake and explosive loads. This is due to modeling complexity and computer costs and to the perception that the results are too cumbersome to be integrated in a design process. This paper illustrates how recent advances in computer and graphics hardware encourage the use of advanced methods in design by making it easy to display snapshots of field quantities such as deformed shapes and distribution of moments and shear. These data show critical parameters for design and their locations. This is in contrast to the usual time history output which, even if it contains the peak response, does little to improve insight into overall response. This paper shows one approach having a beneficial effect on design due to exploiting hardware advances.

There are two approaches to generating and displaying response data in support of structural design. In the first, all computations are performed and postprocessed on a remote mainframe (CRAY or CDC CYBER, for example). User interaction is by telephone through a terminal connected to a modem. Graphical results are sent by mail or images are transmitted over the telephone to be displayed at the user's site. Often, the low data transfer rate associated with this approach impedes the analysis process so that it becomes impractical to vary design parameters quickly.

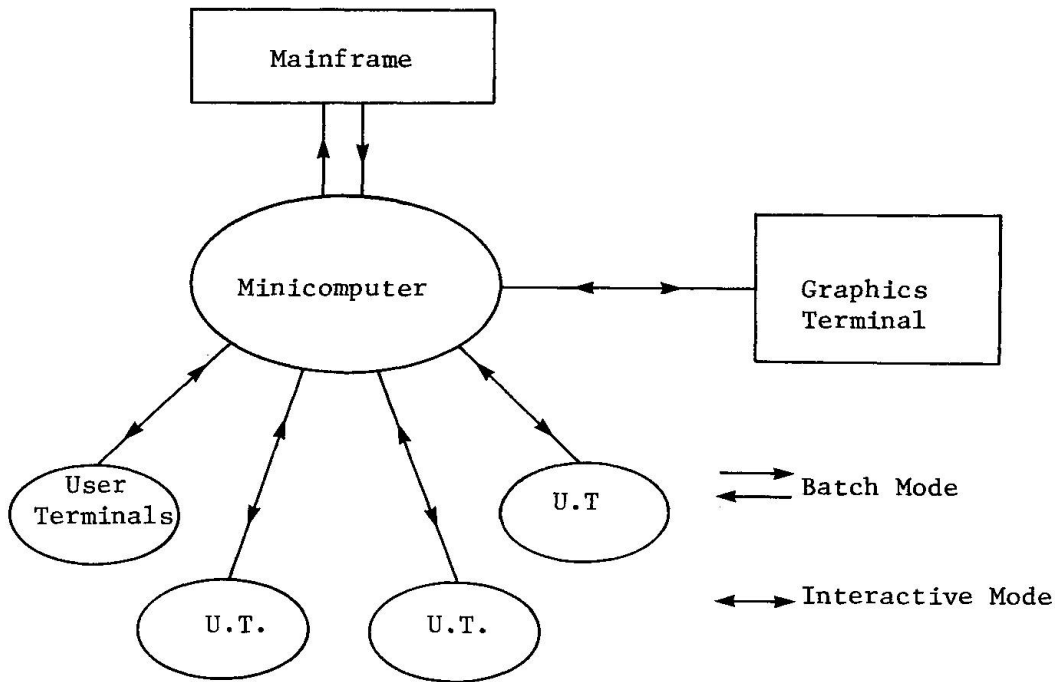
The alternate approach is to maximize analytic work done locally. The largest calculations are still performed at a remote site. However, once computed, the response data are transferred to the in-house computer system using an efficient file transfer protocol (such as HASP). Once local, the response data can be postprocessed and graphically displayed in many different ways without being constrained by telephone transfer rate limitations.

There are two main alternatives in acquiring in-house computer hardware (see Fig. 1). They are a multi-user minicomputer system or a single user workstation system. The minicomputer system is the least expensive approach to support a number of users who routinely create and share data files, perform analyses and postprocess results. Software and peripherals, such as graphics terminals, must be integrated by the user. Typical minicomputer systems which can support this type of work are the VAX and PRIME 32-bit processor machines.

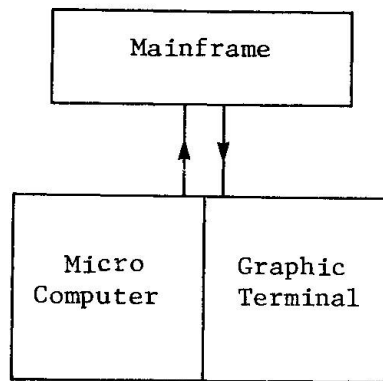
Workstations provide a powerful computing environment dedicated to a single user. These machines are supermicrocomputers which provide integrated data entry, analysis and graphical display. Workstations produced by APOLLO and SUN are typical examples of engineering workstations. Most workstations run UNIX and support FORTRAN. In their simplest configuration, they typically have several megabytes of random access memory, about 60 megabytes of disk storage and special peripherals which support interactive modeling.



All are equipped with high quality graphics monitors having on the order of 1280 x 1024 resolution. A network of workstations which allows file sharing between machines can be achieved using ETHERNET. File servers are also available for these networks.



a. Multi-user minicomputer system



b. Single user workstation

Figure 1. Hardware alternatives which provide design support.



The choice of a minicomputer or workstation approach is dictated by the type of work, workload and number of users which the system is required to support. The workload during both daytime and nighttime hours should be considered in the selection. A workstation gives more power to a single user; the minicomputer distributes resources among a number of users. A minicomputer system is probably more expensive than a single workstation but is less expensive than a number of workstations.

Regardless of which hardware option is adopted, there is incentive to make modeling approximations that focus computer resources on the response of the reinforced concrete members. This is especially so in design support analyses where fast turnaround is needed to assess design alternatives. In analysis of explosive effects, there is often a protective layer of soil or other material which acts to mitigate the shock. It is essential to include the effect of this layer and desirable not to devote much resources to it. Methods for reducing the size of the soil domain in such problems are shown in Fig. 2. The first illustrates a reduced grid coupled with a suitable absorbing boundary. A series of models with progressively reduced soil cover is compared with a simulation standard. Excellent estimates of peak velocity response are obtained for the smallest grid, with a savings in processing time of a factor of order 50 relative to the baseline model. Greater economies are possible in 3-D problems. For flat-roof structures of the type considered in the example given below, there is little interaction between roof and sidewall; in such cases it is possible to reduce the model to a slab with overlying soil [Ref. 1].

The second method for reducing the size of a model is a decoupling approach in which the dynamic soil-structure interface stresses are computed from the following wave-front approximation.

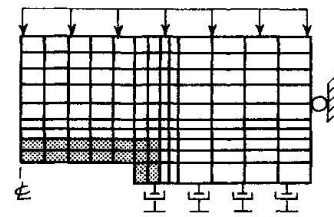
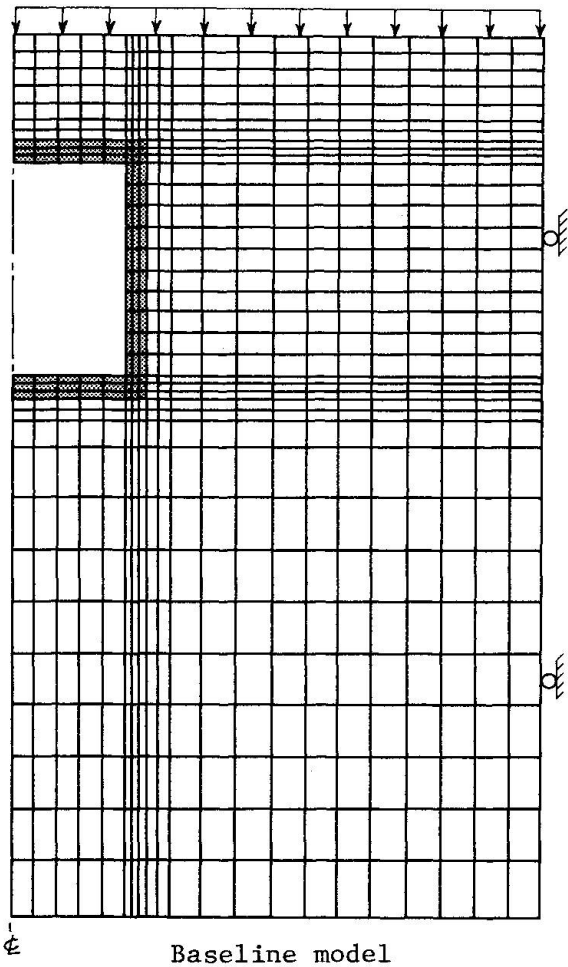
$$\sigma_{\text{int}}(t) = \sigma_{\text{ff}}(t) + \rho c (v_{\text{ff}}(t) - v_{\text{str}}(t))$$

In this case, a preliminary free field analysis is performed to obtain the free field stress and particle velocity components normal to the structure. In highly nonlinear soils, the wave speed c is a function of stress level; a constant value assumed to be equal to the unloading wave speed is usually a satisfactory approximation. Descriptions of decoupling approaches for various applications are given in [Ref. 2, 3, and 4].

Candidate designs which have been evaluated by the procedures described above include shallow buried boxes, cylinders and arches.

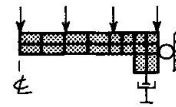
Assessment of candidate designs requires data on spatial variation of stress resultants and deflections which can be displayed as snapshots at various times. Times of interest can be found by searching output files for peaks. Computed peak responses to shock loading often include numerical

overshoot. Post-processing by digital filtering is usually preferable to artificial damping. Reduction in time step is required if such overshoot significantly affect interpretation.



Reduced model with absorbing boundary

$$\sigma = \sigma_{ff} + \rho c \Delta v$$



Reduced model with plane wave approximation for incident load

Figure 2. Finite element models for soil structure interaction and response of roof slab.

2. STRUCTURAL MODELING

2.1 Finite Element

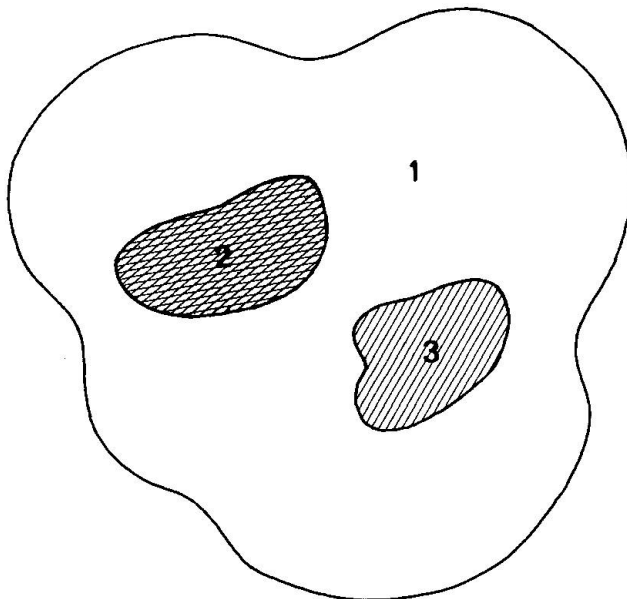
The calculations presented below were performed using FLEX, a 3-D continuum finite element code developed at Weidlinger Associates [Ref. 5]. The standard eight-node isoparametric element, which employs a tri-linear interpolation function to represent the displacement field, is used to model the continuum. The hexahedron with one point quadrature to evaluate the element forces is a computationally efficient scheme for simulating wave propagation in a continuum. For rectangular grids, the approach is equivalent to the staggered grid method used in finite difference codes. The use of single point integration for the stresses results in zero stress deformation modes which, if not constrained, destroy



the solution [Ref. 6]. Control of hourglass instability has been proposed using a number of approaches. One scheme for stabilizing hourglass instability due to Flanagan and Belytschko [Ref. 7] has been implemented in FLEX. This approach isolates the hourglassing modes and provides them with an elastic stiffness to stabilize the mesh.

For dynamic calculations, the time integration algorithm in FLEX is an explicit method based on the central difference operator. This formulation is computationally more efficient than implicit methods for large nonlinear 3-D calculations, especially where small time steps are needed to resolve the steep gradients that occur at wavefronts. Efficiency is further enhanced by using a diagonal lumped mass matrix.

In a typical calculation, the elements vary in size and material type so that the time step required for numerical stability of the solution varies from element to element, (see Fig 3). A subcycling scheme has been implemented in FLEX to use time steps that are close to optimal in different regions. This method can significantly reduce the number of computer operations in the course of a solution. Each region is processed at a time step which is an integer multiple of the smallest time step in the model.



Typical subcycling ratios
for buried reinforced
concrete structure

Region	$\frac{h}{c}$ (time)	Δt (time)
1	10	8
2	5	4
3	1.5	1

h = element size
 c = dilatational wavespeed

Figure 3. Subcycling approach uses integration time step (Δt) appropriate to transit time (h/c) in each region.



A static solution capability based on the conjugate gradient method has been incorporated into FLEX [Ref. 8]. This is an iterative method for solving the equations of equilibrium directly. Prior knowledge of the natural frequencies of the model required for solution by dynamic relaxation is not necessary.

The type of concrete model used predominantly in analysis of protective structures is based on the rate-independent, strain-hardening theory of plasticity. The example which is summarized here is the three-invariant cap model described in [Ref. 9, and 10]. The main features of the model include:

- An ideally plastic failure surface, a function of three stress invariants.
- An isotropically strain-hardening cap which introduces volumetric hysteresis and controls dilatancy (i.e., ratio of major to minor principal inelastic strains) for states of stress inside the failure surface.

The failure surface is in the form of a revised Willam and Warnke failure surface [Ref. 11], (Figs. 4 and 5). Its functional form in terms of stress invariants is given by:

$$f(\sigma_a, \tau_a, \theta) = \frac{\tau_a}{r(\sigma_a, \theta) f_c} - 1 = 0$$

and

$$\sigma_a = \frac{1}{3} (\sigma_1 + \sigma_2 + \sigma_3) = J_1/3$$

$$\tau_a = \sqrt{(2/5)} \sqrt{J_2'} = \sqrt{2/5} \sqrt{(1/2) s_{ij} s_{ij}}$$

$$\cos 3\theta = (3/5) \sqrt{(6/5)} \frac{J_3}{\tau_a^3} = \frac{3\sqrt{3}}{2} \frac{J_3}{(\sqrt{J_2'})^3}$$

$$J_3 = (1/3) s_{ij} s_{jk} s_{kl} ; s_{ij} = \sigma_{ij} - \sigma_a$$

where J_1 is the first invariant of the stresses and hence is the mean pressure; τ_a is related to $\sqrt{J_2'}$, the second invariant of the deviatoric stresses; and θ is the Lode angle related to the third invariant of the deviatoric stresses J_3 and also τ_a .



Here $r(\sigma, \theta)$ represents the cross-sectional shape in the deviatoric plane and is given by

$$r(\sigma_a, \theta) = \frac{2r_2(r_2^2 - r_1^2) \cos\theta + r_2(2r_1 - r_2) \sqrt{4(r_2^2 - r_1^2)\cos^2\theta + 5r_1^2 - 4r_1r_2}}{4(r_2^2 - r_1^2) \cos^2\theta + (r_2 - 2r_1)^2}$$

The functional forms for r_1 and r_2 used for the model are:

$$r_1(\sigma_a) = a_0 - a_1 e^{a_2(\sigma_a/f_c)}$$

$$r_2(\sigma_a) = b_0 - b_1 e^{b_2(\sigma_a/f_c)}$$

The functional form of the cap that intercepts the revised Willam and Warnke failure surface in a plane is

$$f_c = \frac{R^2 - \delta^2}{r^2(L - \delta, \theta) f_c'^2} \frac{\tau_a^2}{f_c'^2} + \frac{(\sigma_a - L)^2}{f_c'^2} - \frac{(X - L)^2}{f_c'^2} = 0$$

where

$$X(\epsilon_v^p) - L(\epsilon_v^p) = -R(\epsilon_v^p)$$

$$\delta = \delta(\epsilon_v^p) \quad ; \quad R = R(\epsilon_v^p)$$

and two forms of hardening rule for the cap have been explored, as follows:

$$\epsilon_v^p = W \left[e^{\bar{D}(X - X_0)} - 1 \right] \quad X = X_0 + C_1 \epsilon_v^p + C_2 \ln \cosh(-C_3 \epsilon_v^p)$$

$$+ C_4 \ln \cosh(-C_5 \epsilon_v^p)$$

The quantities X , L and R , defined in Figs. 3 and 4, represent the intercept on the hydrostatic axis and maximum value of σ_a for the semi-major axis of the elliptical variation of the cap cross section with regard to σ . X_0 defines the initial position of the cap. The quantities W and D (or C_1 through C_5) define the hydrostatic hardening and are fit to hydrostatic stress-strain curves. The constitutive laws invoke the conventional flow rules of plasticity theory and the yield and loading criterion.

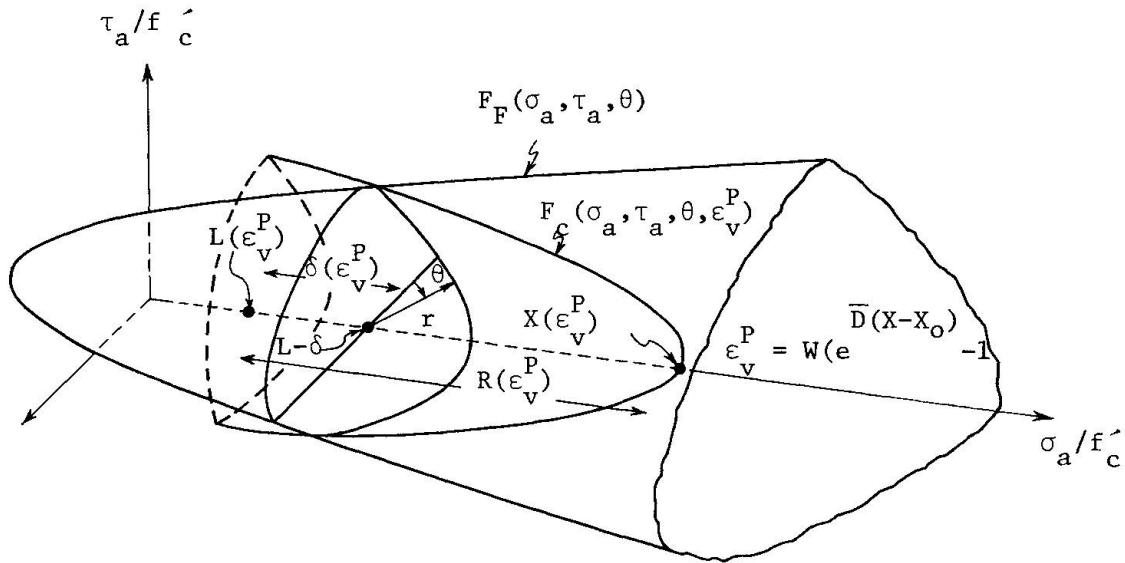
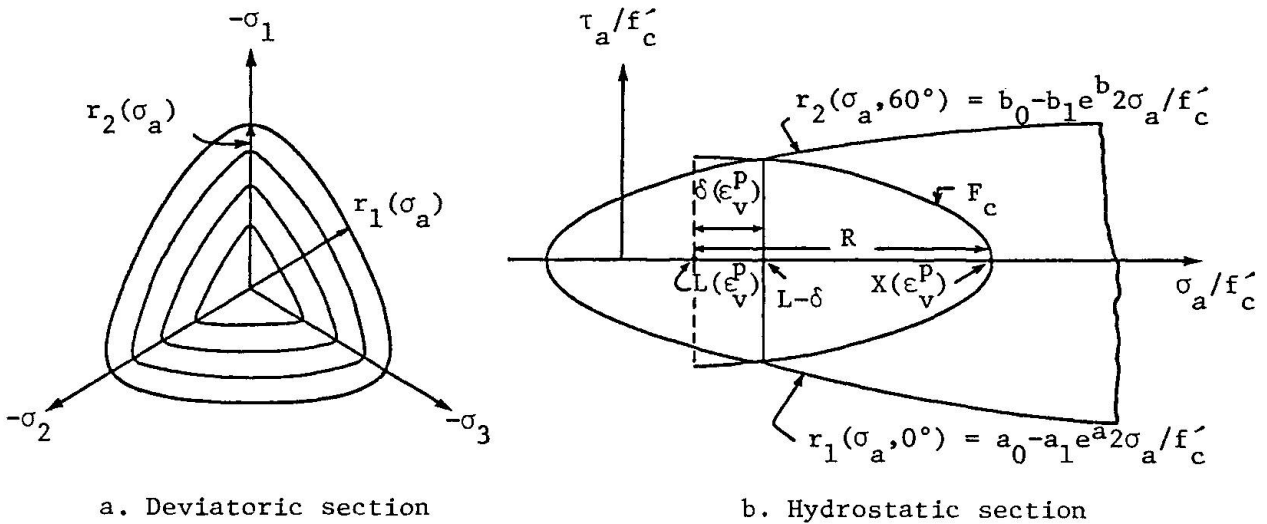


Figure 4. Configuration of cap in relation to failure surface.



a. Deviatoric section

b. Hydrostatic section

Figure 5. Cross section of cap and failure surface.

The enhancement of concrete strength due to strain rate effects in a rate-independent model requires the analyst to estimate the anticipated strain rate induced by the primary loading in the calculation. An enhancement factor is obtained from laboratory tests performed at a comparable strain rate. The initial concrete strength in the calculation is then adjusted by the enhancement factor. Modifications, similar to the viscoplastic model of Perzyna [Ref. 12] are being implemented to eliminate the ad hoc procedure approach, the rate of plastic straining is assumed to be proportional to the difference between a stress function and a quasi-static yield limit. This leads to stress relaxation from a dynamically induced peak back to the quasi-static



yield surface at a rate that depends on the strain rate. The behavior of plain concrete is typically brittle at low confining pressures and becomes increasingly ductile with increasing confinement. The ductility inherent to plastic and viscoplastic material models is an appropriate approximation at high confining stresses, but at low confinement tends to overpredict the residual strength. The development of a rate-dependent, damage accumulation model is currently underway to address strain softening of plain concrete. The model is based on the concept of irreversible, isotropic damage. As a material is loaded into the softening range, spherical voids are assumed to form. Damage is defined as the ratio of these voids to the original volume. Damage is assumed to accumulate whenever the effective stress lies on or above the yield surface; that is, damage accumulation coincides with volumetric dilation. In spite of the simplifying assumptions required, this model is viewed as a significant improvement over unlimited ductility.

Modeling of the reinforcing bars is accomplished by the use of an explicit rebar element. Figure 6 shows a typical reinforcing detail for a structure and the modeling approximation. The strain in each bar is assumed to be equal to the strain in the continuum element evaluated at the centroid, and in the direction of the bar axis. The bar is assumed to be elastic, ideally plastic; the stress is uniquely a function of axial strain and stress history. Ideal bond conditions are assumed between the plain concrete and reinforcing bars. The primary goal of modeling reinforcing in this manner is to represent the confining effect of steel bars on plain concrete.

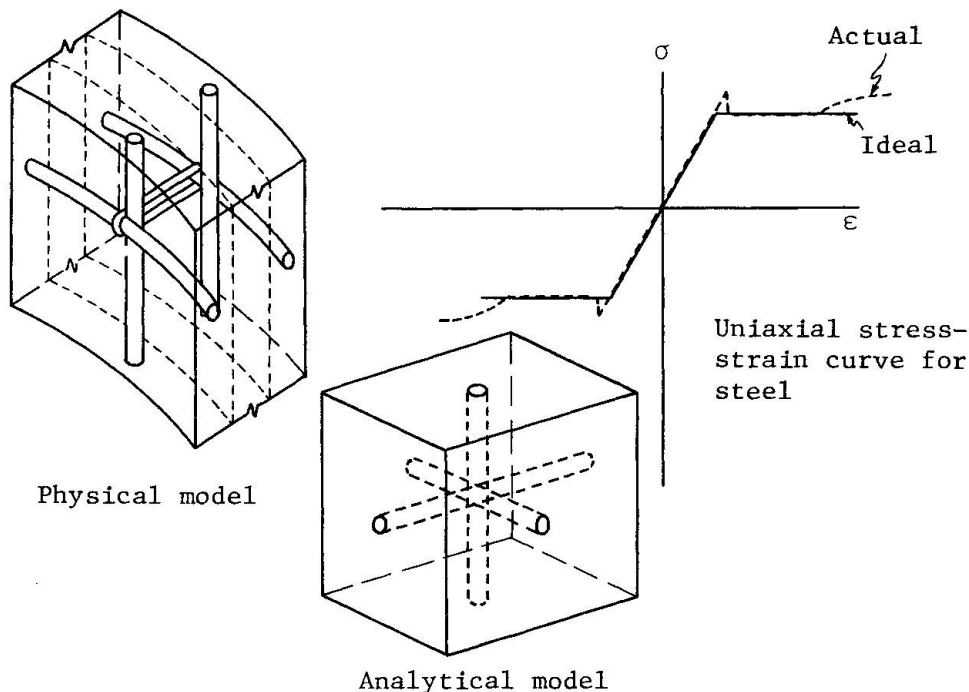


Figure 6.



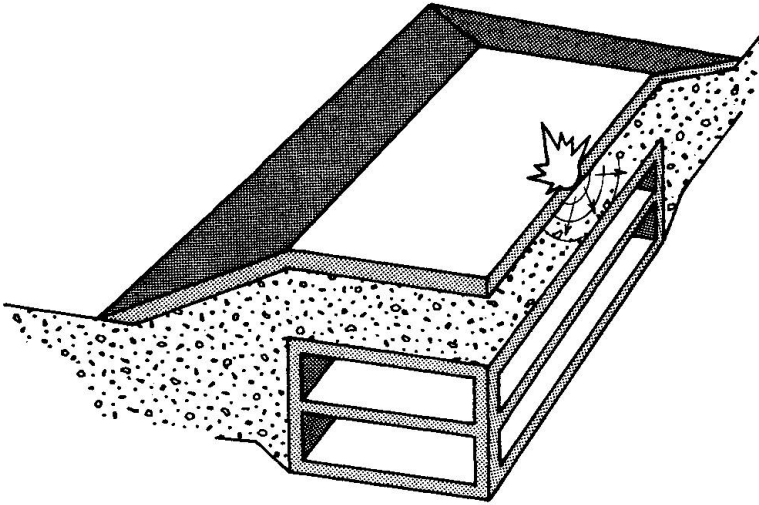
This model accurately predicts the response of designs that survive explosive effects with light to moderate damage. Predictions of failure require interpretation based on extensive previous correlation with field test data.

3. EXAMPLE

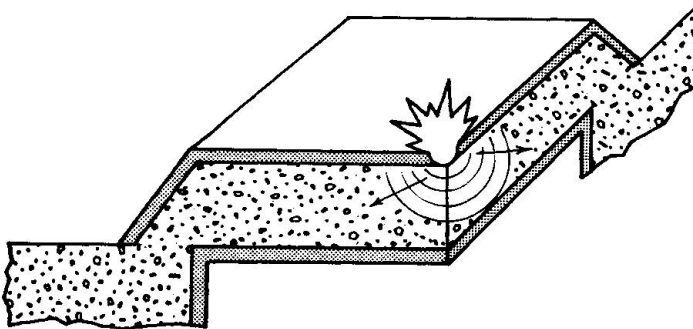
Calculations supporting the design of a complex structure rarely consider the entire configuration. Typically, the design is decomposed into an assembly of components which are analyzed individually. The detail to which these structural elements are modeled depend on requirements to characterize the role of the element in the physical structure as well as the number of design parameters to be considered. Figure 7 describes the evolution of a computational model from the complete configuration to a bare roof slab subjected to a loading obtained from a simplified soil/structure interaction algorithm. In this case, the design of the roof slab has been completed, and a 3-D finite element model was constructed to perform validation calculations for two threat scenarios. The threats consisted of detonations on the burster slab above centerspan ($x = 0, y = 0$), (Case 1), and above the center of the short span near the long span support ($x = 0, y = 10l_y/11$), (Case 2). The initial conditions for the dynamic analyses were obtained from a static calculation of the slab loaded by the weight of the burster slab and overburden material. The decoupling scheme, described in section 1, was employed to evaluate the soil/structure loading. The energy coupling of the detonation into the ground and ground shock approximations used for the free-field definition were obtained from Ref. 13. The inherent symmetry of the roof slab and the location of the bursts permitted reduction of the required model to one-quarter of the roof slab. The discretization of the slab consisted of five-single-integration point elements through the thickness, and an overall element aspect ratio of one; resulting in a total of 12,615 elements. In an effort to obtain an accurate representation of the bending restraint at the wall without modeling the wall, the portion of the roof over the wall was included in the model. A horizontal roller support condition was then applied to the bearing surface, which eliminates wall rotations and displacement. An additional constraint, in which each row of nodes along exterior vertical edge of the slab were permitted to translate rigidly with no rotation, was imposed. This boundary condition prevents an unrealistic build-up of in-plane thrusts which artificially enhance the moment and shear capabilities of the slab, that full in-plane and rotational fixity would produce. The plain concrete is modeled using the rate independent, strain hardening version of the concrete model. The reinforcing bars are modeled explicitly using the rebar elements. The simulation output consists of a minimal number of velocity histories used primarily for diagnostic purposes, and a large number of displacement and resultant force snapshots, used for field display useful to



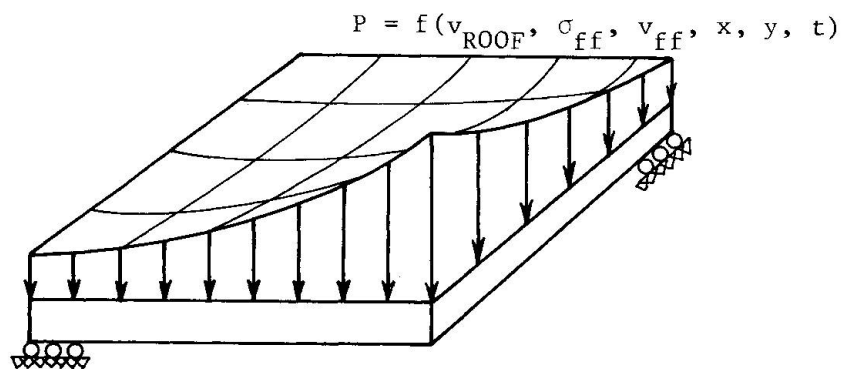
the designer. The model requires approximately one million words of central memory and 6 cp-minutes per 10 ms of structural response on a CRAY-1 computer. Peak response occurs at about 20 ms for the cases presented here.



a. One-quarter of the structure.

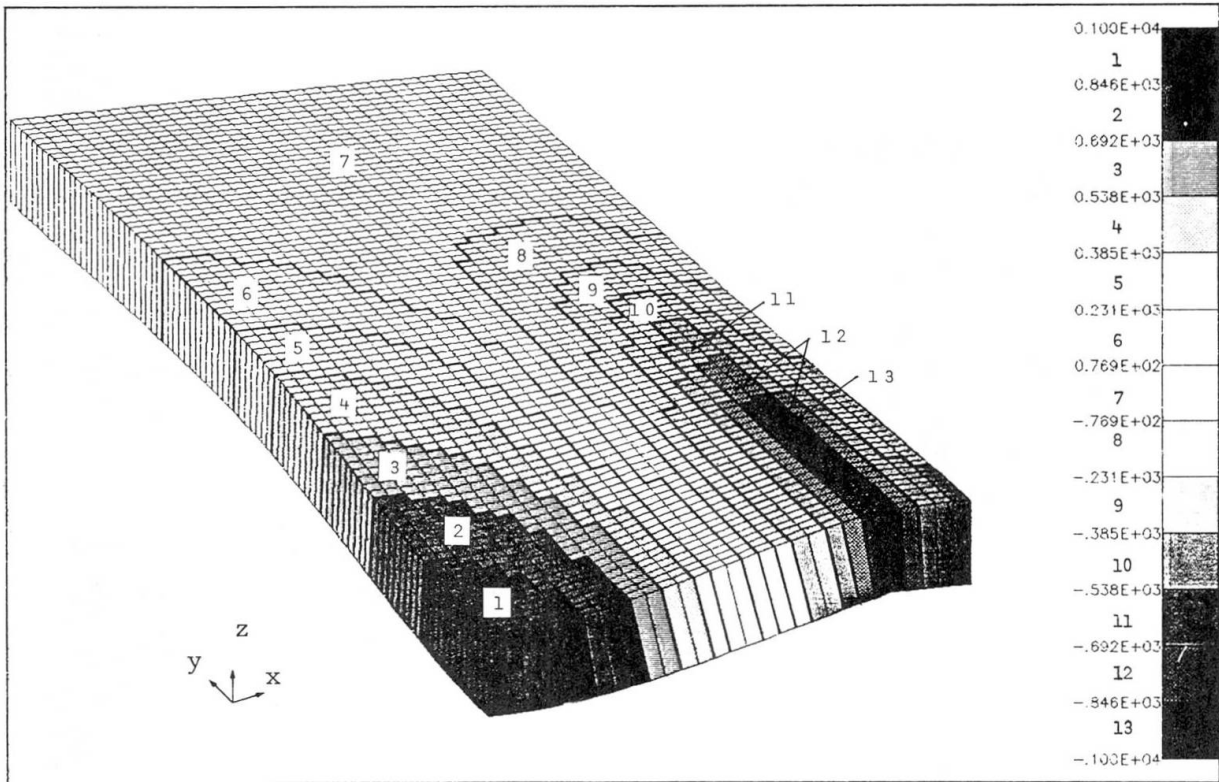


b. Roof slab including burster slab and overbursts

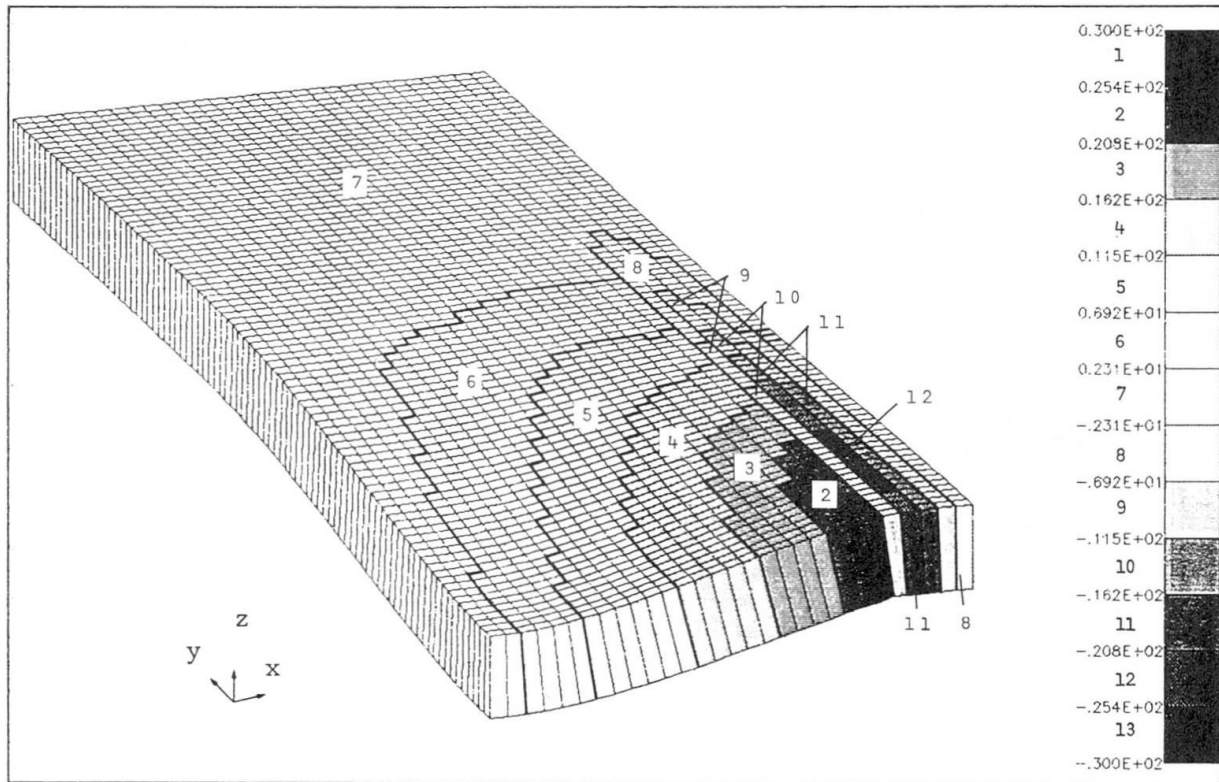


c. Roof slab model and semi-empirical interaction model

Figure 7.

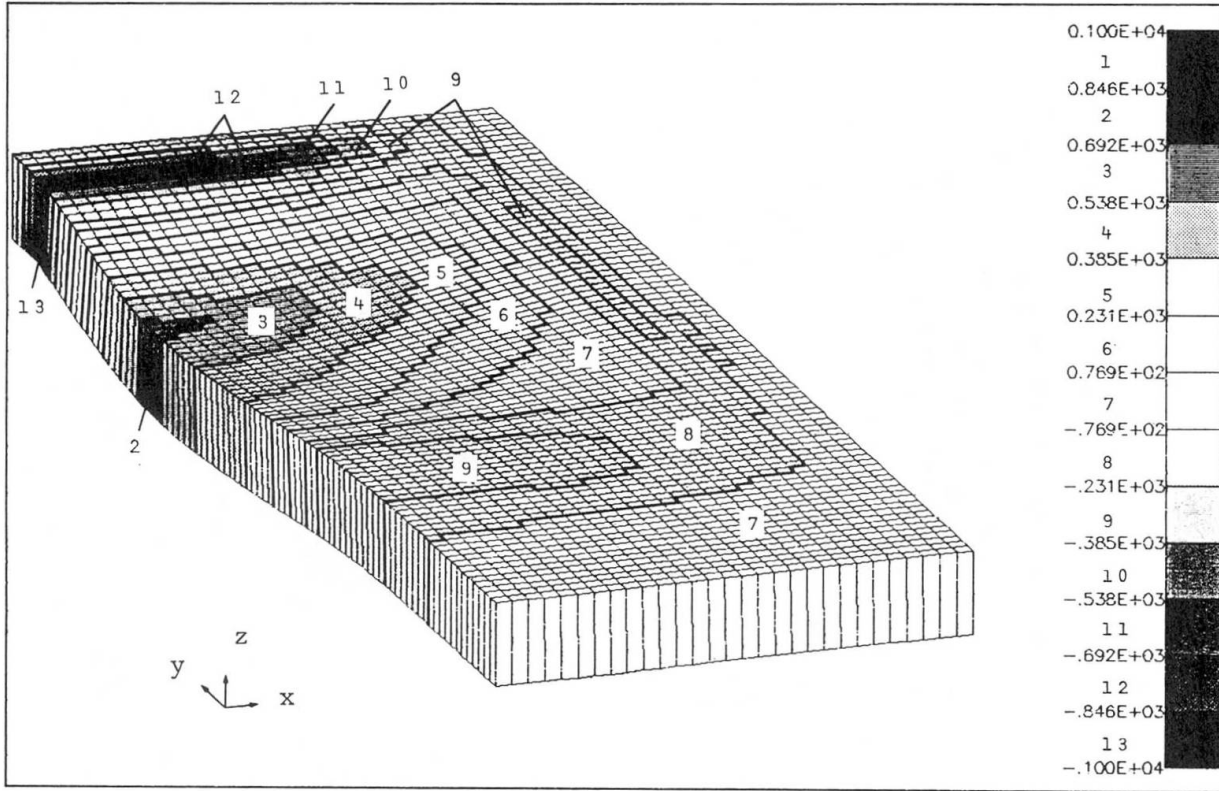


Short span moments (M_{yy}) for Case 1 at 20 ms.

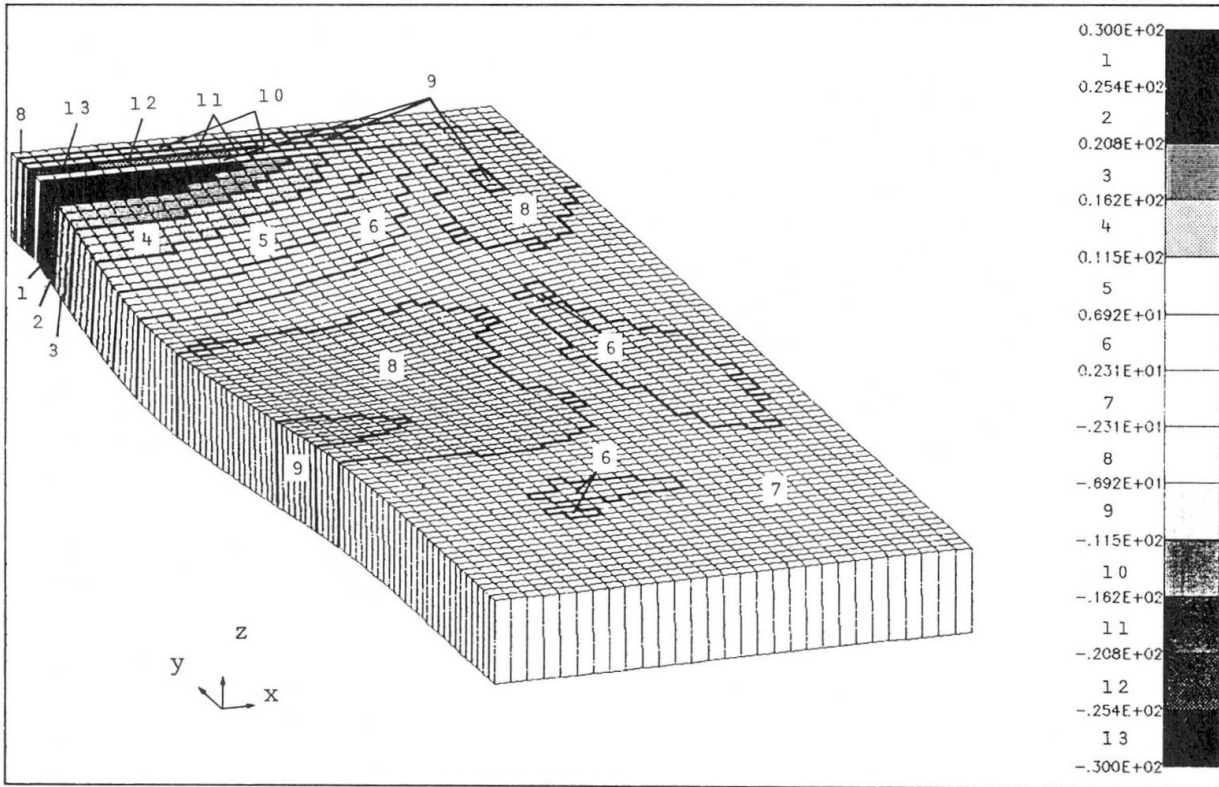


Short span shear (V_{xz}) for Case 1 at 20 ms.

Figure 8.



Long span moments (M_{xx}) for Case 2 at 20 ms.



Long span shear (V_{yz}) for Case 2 at 20 ms.

Figure 9.

Figure 8 shows the short span bending moments and shear forces in the slab near peak response for Case 1. The rapid decay of these quantities in the long direction indicates one-way response of the roof. The superposition of the bending moments and shears on the deformed mesh provide the designer with a near complete picture of the structural response. The advantages of viewing a few of these snapshots at discrete times over examining a large number of history plots is readily apparent. The short span response for Case 2 is comparable in magnitude to Case 1 with the peaks occurring directly below the burst. Figure 9, which shows the bending moment and shear in the long direction, indicates the degree of two-way action occurring for this case. A locus of critical sections for the roof slab can be deduced by combining the results of these attacked scenarios.

4. SUMMARY

This paper discusses how nonlinear dynamic finite element analysis capabilities for reinforced concrete structures can be accessible to a design office. The hardware alternatives considered ranged from total dependence on a remote mainframe to a configuration which employs a complement of small local as well as remote computers. The local system is used for pre- and postprocessing, while the analysis itself is performed remotely. The local systems discussed included mini-computers suitable for supporting a large number of users and work stations for single users which could be networked to accommodate a multi-user environment. All configurations considered include a high resolution color graphics terminal. The feature enables the analyst to view color-coded snapshots of field quantities, such as stress, strain, forces, and moments, superimposed on deformed meshes. This provides a powerful tool to the designer who can readily indentify the magnitude and location of critical response quantities.

Given this hardware environment, detailed design support calculations can be performed and easily interpreted. A continuum code, FLEX, which is particularly suited to this class of problems is presented. An eight-noded, single integration point hexahedron, which is explicitly integrated in time, provides the foundation of the code. The plain concrete is modeled using a three invariant version of the cap model. Model development efforts are currently directed towards including strain rate effects and strain softening. A rebar element for explicitly modeling the reinforcing bars, completes the features necessary for the modeling reinforced concrete structures.

The impact of these hardware and software advances are demonstrated in the analyses of a 3-D roof slab model subjected to a blast loading. The effectiveness of these improvements is evident in the ease of assessing the structural response from a few selected displays of field quantities.



REFERENCES

1. WONG, F. S. and WEIDLINGER, P., "Design of Underground Shelter Including Soil-Structure Interaction Effects", Proc of a Symposium on Interaction of Non Nuclear Munitions with Structures, U.S. Air Force Academy, May 10-13, 1983.
2. NELSON, I. and ISENBERG, J., "Soil Island Approach to Structure/Media Interaction", Numerical Methods in Geomechanics, CS Desai (Ed) Proc 2nd International Conference on Numerical Methods in Geomechanics, Virginia Polytechnic Institute and State University, June 1976, p41-57.
3. LYSMER, J. and KUHLEMEYER, R. L., "Finite Element Dynamic Model for Infinite Media", J. Eng. Mech. Div., Proc ASCE V95 No.EM4, August 1969, p859-877
4. SANDLER I, "A Method of Successive Approximations for Structure Interaction Problems", Computational Methods for Infinite Domain Media-Structure Interaction, AMD-Vol. 46, Presented at The Winter Meeting of ASME, November 1981.
5. VAUGHAN, D. K., "FLEX Users Manual", Weidlinger Associates WA-MP-UG 8298 December 1982, Revised March 1985
6. IRONS, B. and AHMAD, S., "Techniques of Finite Elements", Ellis Horwood, Chichester, England, 1980.
7. FLANAGAN, D. P and BELYTSCHKO, T., "A Uniform Strain Hexahedron and Quadrilateral with Orthogonal Hourglass Control", International Journal for Numerical Methods in Engineering, Vol. 17, p679-706, 1981.
8. PILAND, T. J., ISENBERG, J. and GHABOUSSI, J., "Finite Element Analysis of Misty Rain Tunnel Intersection", Weidlinger Associates DNA Report R8626, May 1986.
9. LEVINE, H. S., "A Two-Surface Plastic and Microcracking Model for Plain Concrete", Nonlinear Numerical Analysis of Reinforced Concrete, Winter Annual Meeting ASME, Phoenix, AZ, November 14-19, 1982.
10. LEVINE, H. S. and MOULD, J. C., "A Three-Invariant Cap Model for Concrete Soil and Rock: Computational Aspects", ASME/ASCE Summer Mechanics Conference, Albuquerque, NM, June 1985.
11. WILLAM, K. J. and WARNKE, E. P., "Constitutive Model for the Triaxial Behavior of Concrete", IABSE Seminar on Concrete Structure Subjected to Triaxial Stresses, Paper III-1, Instituto Specimentali Modelli e Strutture, Bergamo, Italy, May 1974
12. PERZYNA, P., "The Constitutive Equations for Rate Sensitive Plastic Materials", Quarterly Appl. Math., Vol. 20, Nov. 4, 1963.
13. "Fundamentals of Protective Design for Conventional Weapons", Structures Laboratory, Department of Army, Waterways Experimental Station, Corps of Engineers, Vicksburg, Mississippi, July 1984